A Rapid Synthesis of Hf-Beta Zeolite as Highly Active Catalyst for Meerwein-Ponndorf-Verley Reduction by Controlling Water Content of Precursor Gel

Taichi Nakamura,[1] Yuichi Kamiya[2], and Ryoichi Otomo[2, *]

[1]Graduate School of Environmental Science, and [2]Faculty of Environmental Earth Science, Hokkaido University, Kita 10 Nishi 5, Kita-ku, Sapporo 060-0810, Japan.

*Corresponding author: Dr. Ryoichi Otomo

Tel: +81-11-706-2259, E-mail: otomo@ees.hokudai.ac.jp

Abstract

Hf-Beta is a promisingly active Lewis acid catalyst for Meerwein-Ponndorf-Verley (MPV) reduction and other important organic reactions. However, the conventional hydrothermal synthesis of Hf-Beta inevitably requires the troublesome procedure for hydrolysis of tetraalkoxysilane and the long period to complete crystallization. In the present study, we applied a synthetic approach of reducing water content of precursor gel and succeeded in considerably shortening the period for crystallization of Hf-Beta using fumed silica as silicon source. By using precursor gel with H_2O/SiO_2 = 1.4 – 7.6, effect of water content of precursor gel on the crystallization of Hf-Beta, the incorporation of Hf into the zeolite framework, and the catalytic performance were thoroughly investigated. Low water content was favorable for accelerating the crystallization, but unfavorable for the incorporation of Hf into the zeolite framework, resulting in poor catalytic activity. With the assistance of seed crystal, Hf-Beta with a relatively large amount of framework Hf was obtained from the precursor gel with H_2O/SiO_2 = 6.4 in 24 h. Hf-Beta synthesized in this way showed higher catalytic activity for MPV reduction than Hf-Beta as well as Zr-, and Sn-Beta synthesized by the conventional hydrothermal method.

Keywords

Hf-Beta; Lewis Acid; Metallosilicate; MPV Reduction; Zeolite

1. Introduction

MPV reduction is a useful reaction to produce alcohols from aldehydes or ketones under mild conditions. Traditionally, aluminum alkoxides [1-3] and metal complexes [3,4] are used as homogeneous Lewis acid catalysts for MPV reduction. Various types of heterogeneous catalysts have been studied for MPV reduction such as layered double hydroxides [5], metal oxides [6,7], supported metal alkoxides [3,8], and zeolites [9-20]. Of these materials, metallosilicate Beta zeolites with ***BEA**-type structure containing tetravalent heteroatoms such as Ti^{4+}, Zr^{4+}, Sn^{4+}, and Hf^{4+} have emerged as highly active Lewis acid catalysts [10,12-20] with shape selectivity [10,12-16], tolerance against water [10,14], and recyclability [14]. In the last several years, Hf-Beta has been reported to show higher catalytic activity than metallosilicate analogues with Ti, Zr, and Sn for the MPV reduction of specific substrates [17-20].

Almost all of Hf-Beta samples reported so far were synthesized by the conventional hydrothermal method with hydrofluoric acid as mineralizing agent [17-20]. The conventional synthesis method successfully gives highly crystalline Hf-Beta with high catalytic activity, whereas it requires long period (several weeks) to complete the crystallization of Hf-Beta. In addition, when silicon alkoxide such as tetraethyl orthosilicate is used as silicon source, the alcohol produced by its hydrolysis must be removed from the precursor gel. To our knowledge, there has been only one alternative method, in which Hf-Beta was prepared by impregnating the Hf complex on dealuminated Beta [21]. In this method, extra-framework Hf species were generated, and post-synthetic acid treatment with concentrated nitric acid was required to remove them.

While there is limited variation of method for synthesis of Hf-Beta, several advanced methods have been developed for short-term synthesis of the other metallosilicate Beta in simple manners [22-31].For example, several groups reported the reduction of crystallization period for synthesis of Sn-Beta by decreasing the water content of precursor gel [23,24,26-28,30,31]. Yakimov et al. [26] reported that for synthesis of Sn-Beta with Si/Sn = 100, the crystallization period was reduced from 60 to 16 days by decreasing H_2O/SiO_2 ratio in precursor gel from 6.8 to 5.6 and that the decrease in the water content did not affect the chemical state of Sn in the framework of Sn-Beta. Yang et al. [31] investigated in detail the crystallization profile and evolution of Lewis acid sites for Sn-Beta using precursor gel with H_2O/SiO_2 = 4.5 and 7.5. The use of the precursor gel with lower water content resulted in faster crystallization and the number of Lewis acid sites for fully crystallized samples did not depend on the water content. Application of these methods to other zeolites is expected to bring shorter synthesis period and simplified procedure. However, the effect of water on the chemical state of heteroatoms in final products can vary from metal to metal, and the developed methods cannot always be applied to other metals by simply changing the metal source.

In the present study, Hf-Beta was synthesized from precursor gel with different H_2O/SiO_2 ratios using fumed silica as silicon source. Effects of water content of precursor gel on the crystallization of zeolite and the incorporation of Hf into zeolite framework were thoroughly investigated. By using precursor gel with a low H_2O/SiO_2 ratio, rapid crystallization was achieved, but the amount of Hf incorporated into the zeolite framework was only little. At the optimal H_2O/SiO_2 ratio, Hf-Beta rich in framework Hf was successfully synthesized in a short period with the assistance

of seed crystal. In addition, Hf-Beta synthesized in this way showed higher catalytic activity for MPV reduction than Hf-Beta and other metallosilicate zeolites that were synthesized by the conventional hydrothermal method.

2. Experimental

2.1. Materials

Tetraethylammonium hydroxide (TEAOH, 35 wt.% aqueous solution), hafnium chloride ($HfCl_4$, 98 wt.%), and furfural (≥99.0%) were purchased from Sigma-Aldrich. Ammonium fluoride (NH_4F, 97%), hydrofluoric acid (47 wt.%), 2-propanol (98%), and *o*-xylene (98%) were purchased from FUJIFILM Wako Pure Chemical. 4-Methylcyclohexanone (98%), cinnamaldehyde (≥98.0%), and acetophenone (≥98.5%) were purchased from TCI. Fumed silica Aerosil® 300 was purchased from NIPPON AEROSIL. Deuterated acetonitrile (CD_3CN, 99.8% deuterated) was purchased from Cambridge Isotope Laboratories. Al-Beta (CP-814E with Si/Al = 12.5) was purchased from Zeolyst International.

2.2. Synthesis of Hf-Beta

Hf-Beta was synthesized by hydrothermal treatment of aqueous precursor gel, typically as follows. 0.107 g of $HfCl_4$ was added to 7.56 g of TEAOH solution in 50 mL Teflon beaker, and the resulting mixture was stirred at 60 °C for 1 h. After cooling the mixture to ambient temperature, 2.0 g of fumed silica was added with stirring. At this point, seed crystal corresponding to 1 wt. % of SiO_2

was optionally added. The resulting suspension was further stirred at ambient temperature for 2 h. Then, 0.67 g of NH_4F was added to the suspension. Considering the water contained in fumed silica (1.9 wt.%), the resulting gel had a molar composition of 1.0 SiO_2: 0.55 TEAOH: 0.01 $HfCl_4$: 0.55 NH_4F: 8.7 H_2O. To obtain precursor gel with lower water content, the gel was heated at 60 °C to evaporate desired amount of water. The weight of the gel was measured before and after the heating, and the amount of water in the final precursor gel was estimated assuming that the weight loss during the heating was due to the evaporation of water. For several representative precursor gel samples, the actual water content was measured by the thermogravimetric analysis, and it was confirmed that the above estimation was correct. The volume of precursor gel with H_2O/SiO_2 = 6.4 and 1.4 was 7.5 and 4.6 mL, respectively. The precursor gel was transferred to a 100 mL Teflon-lined stainless-steel autoclave. The crystallization was done by heating the autoclave under static conditions at 180 °C for a set period. After the crystallization, the solid sample was recovered by filtration, washed with ethanol and Milli-Q water, and finally dried at 60 °C overnight. The as-synthesized sample was calcined in air at 650 °C for 6 h. Samples for different crystallization periods were obtained in separate synthesis batches following the aforementioned procedure.

The seed crystal was prepared by dealumination of the commercially available Al-Beta. 10 g of Al-Beta was treated in 500 mL of 7.2 mol L^{-1} HNO_3 solution at 80 °C for 24 h. The solid was recovered by suction filtration, washed with Milli-Q water, and dried at 60 °C overnight. Si/Al ratio of the dealuminated Beta (DeAl-Beta) was determined to be higher than 1000 by ICP-AES.

As a comparison, Hf-, Zr-, and Sn-Beta were prepared by the conventional hydrothermal

method with hydrofluoric acid [32], and are denoted as Hf-HF, Zr-HF, and Sn-HF, respectively. HfO_2/Si-Beta was prepared by calcining the mixture of HfO_2 and Si-Beta, which was prepared by the conventional hydrothermal method.

2.3. Characterization

Powder XRD patterns of samples were collected on a Rigaku MiniFlex diffractometer with Cu Kα radiation (30 kV, 15 mA, λ = 0.154 nm) at a step width of 0.02°. Nitrogen sorption isotherms were measured on a MicrotracBEL BEL-mini analyzer at -196 °C. Prior to the measurement, samples were pretreated in nitrogen flow (50 mL min^{-1}) at 400 °C for 1 h. Specific surface area was calculated by the Brunauer-Emmett-Teller (BET) method. Morphology of samples was observed by a FE-SEM using Hitachi S-4800 microscope at an acceleration voltage of 1 kV. Elemental analysis of solid samples was performed by ICP-AES using a Shimadzu ICPE-9000 analyzer. 10 mg of samples were added to 5 mL of 1 M KOH aqueous solution and heated at 100 °C for 30 min. The resulting solution was diluted with Milli-Q water and analyzed.

Acid properties of samples were examined by FT-IR spectroscopy with CD_3CN as a probe molecule. FT-IR measurement was carried out on a JASCO FT/IR-4600 with a TGS detector with 64 scans and 2 cm^{-1} resolution in the range of 4000 – 400 cm^{-1}. A powder sample (45 mg) was pelletized to a self-supporting disk with diameter of 2 cm and placed in a quartz IR cell with CaF_2 optical windows. The sample disk was pretreated at 400 °C for 1 h under vacuum. After the sample was cooled to 30 °C, the first spectrum of the bare sample was recorded. A dose of CD_3CN with

predetermined pressure of 5 Pa was introduced into the cell. After the pressure became constant, a spectrum was recorded. Then, CD_3CN was evacuated. This procedure was repeated with the dosing pressure of CD_3CN increased up to 2000 Pa. Here, difference spectra between the first spectrum and the spectra after dosing CD_3CN at certain pressure are shown. To compare the spectra quantitatively, spectra were normalized by using absorption bands of framework vibration at 1500 – 2100 cm^{-1}.

2.4. Catalytic reaction

Catalytic performance of samples was evaluated in MPV reduction of various ketones and aldehydes such as 4-methylcyclohexanone (MCHOne), furfural, cinnamaldehyde, and acetophenone with 2-propanol (2-PrOH). Typically, MPV reduction of MCHOne with 2-PrOH was conducted as follows. A powder catalyst (25 mg) was added to 10 mL of 2-PrOH solution of MCHOne (0.5 mol L^{-1}) and *o*-xylene (internal standard, 0.015 mol L^{-1}) in a test tube. The resulting suspension was heated at 70 °C with stirring for 1 h. The solid catalyst was separated by centrifugation and the supernatant solution was analyzed on a Shimadzu GC-2025 gas chromatograph equipped with a frame ionization detector and a capillary column (SH-Rtx-Wax, 30 m × 0.25 mm × 0.5 μm, Shimadzu). Substrate conversion and products yield were calculated from pre-drawn calibration curves using *o*-xylene as an internal standard.

3. Results and Discussion

3.1. Influence of Water Content of Precursor Gel on Crystallization, Hf Incorporation

and Catalytic Activity

Influence of water content of precursor gel on crystallization of Hf-Beta was investigated by heating precursor gel with H_2O/SiO_2 = 1.4 – 7.6 at 180 °C for 72 h. Fig. 1 shows XRD patterns of samples calcined at 650 °C. The products obtained from the precursor gel with H_2O/SiO_2 = 1.4 – 6.4 showed typical diffraction patterns assignable to ***BEA**-type structure and no impurity phase was found. From the precursor gel with H_2O/SiO_2 = 6.8 and 7.6, amorphous products were obtained, indicating that for the precursor gel with the high water content, crystallization did not proceed sufficiently under the present conditions. By using the precursor gel with low water content, Hf-Beta was successfully synthesized in far shorter period than that required for the conventional method typically using the precursor gel with $H_2O/SiO_2 \geq 7.5$ [17-20].

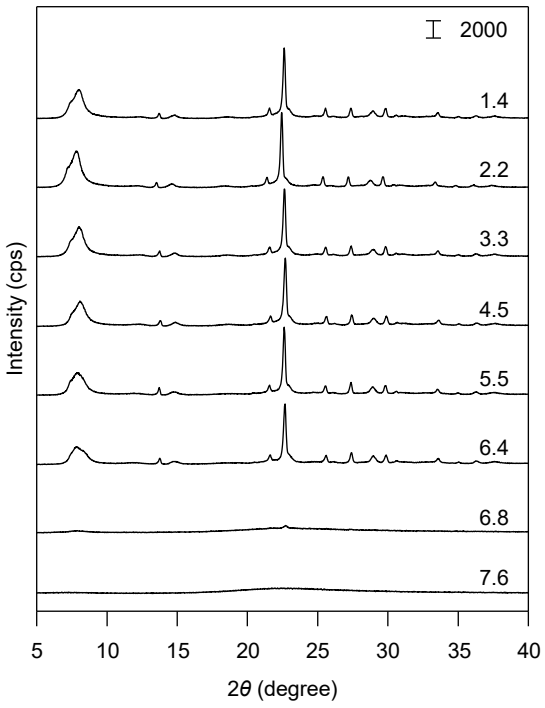

Fig. 1. XRD patterns of calcined samples synthesized from precursor gel with different water content. The numbers in the figure represent H_2O/SiO_2 ratios of precursor gel.

Fig. 2 shows the relationship between water content of precursor gel and Hf content, and catalytic activity for MPV reduction of MCHOne with 2-PrOH. Please note that the amorphous products obtained from the precursor gel with H_2O/SiO_2 = 6.8 and 7.6 are excluded. The Hf content increased as the water content increased, implying that water in precursor gel played an important role in the incorporation of Hf into zeolite framework. The catalytic activity increased as the Hf content increased. It was found that the precursor gel with high water content was necessary to synthesize highly active Hf-Beta with high Hf content.

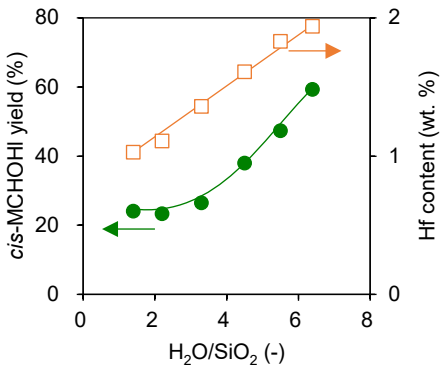

Fig. 2. Influence of water content of precursor gel on Hf content (□) and catalytic activity (●) of Hf-Beta. *cis*-MCHOH = *cis*-4-methylcyclohexanol.

3.2. Crystallization Process of Hf-Beta from Precursor Gel with H_2O/SiO_2 = 1.4 and 6.4

The precursor gel with H_2O/SiO_2 = 1.4 and 6.4, selected as low and high water content system, respectively, was heated at 180 °C for different periods to follow crystallization process of

Hf-Beta. In the synthesis using the precursor gel with H_2O/SiO_2 = 1.4, the diffraction lines of the (101) and (302) planes of the ***BEA**-type structure were observed at 7.9° and 22.7°, respectively, even at 8 h (Fig. 3a). Upon extending the period to 16 h, the diffraction line intensity increased sharply. No further change was found in the diffraction pattern with further extension to 72 h. On the other hand, for samples from the precursor gel with H_2O/SiO_2 = 6.4, very weak diffraction lines first appeared at 24 h, and a highly crystalline sample was finally obtained in 72 h (Fig. 3b). For both systems, no crystalline impurity phase was found. Hereafter, the samples will be denoted as Hf-*x*-*y*, where *x* and *y* represent H_2O/SiO_2 ratio of precursor gel and crystallization period, respectively.

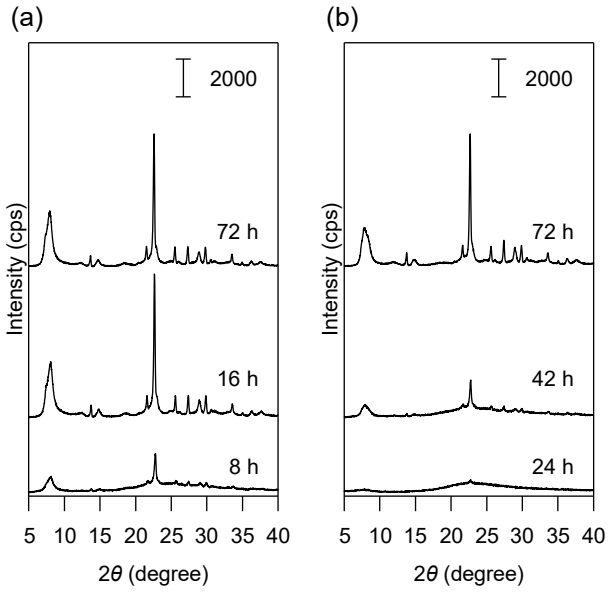

Fig. 3. XRD patterns of calcined samples synthesized from precursor gel with H_2O/SiO_2 = (a) 1.4 and (b) 6.4 at different crystallization periods.

Relative crystallinity of samples from the precursor gel with H_2O/SiO_2 = 1.4 and 6.4 were calculated based on the diffraction line intensities of Hf-1.4-16 and Hf-6.4-72, respectively (Fig. 4a).

For both systems, an induction period was observed before steep increase in the relative crystallinity. A very short induction period of ~4 h was observed for H_2O/SiO_2 = 1.4, while a relatively long induction period of ~30 h was found for H_2O/SiO_2 = 6.4. When the relative crystallinity increased, there was also a difference in the slope of the curve between the two systems, and the crystallization proceeded more rapidly for H_2O/SiO_2 = 1.4. The relative crystallinity reached 90% at 16 and 72 h for H_2O/SiO_2 = 1.4 and 6.4, respectively. Weight yield of the solid products was ~90% regardless of the water content of precursor gel and the crystallization period.

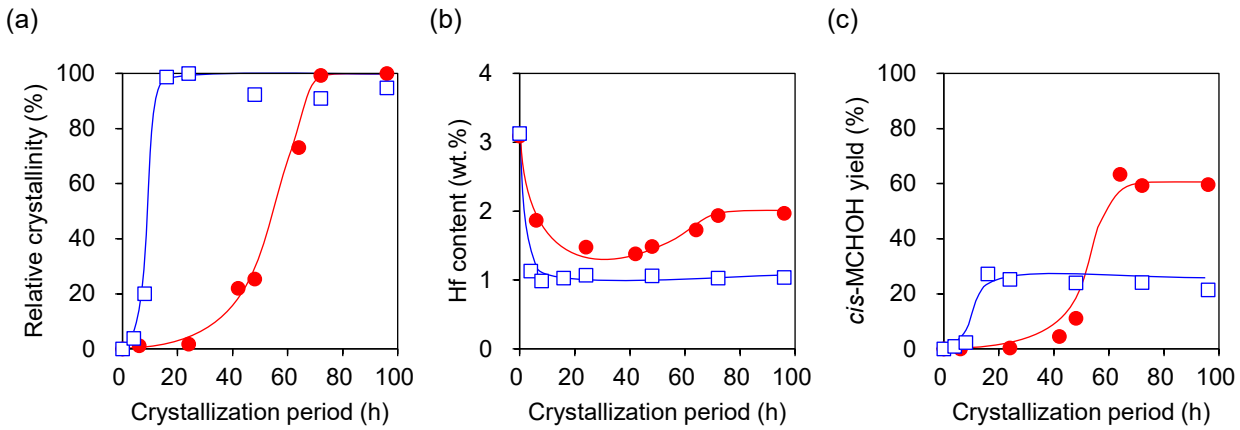

Fig. 4. Temporal changes in (a) relative crystallinity, (b) Hf content, and (c) catalytic activity for MPV reduction in course of crystallization of Hf-Beta from precursor gel with H_2O/SiO_2 = 1.4 (□) and 6.4 (●). *cis*-MCHOH = *cis*-4-methylcyclohexanol.

Fig. 4b shows variation of Hf content in the samples synthesized in both systems at different crystallization periods. Both types of precursor gel with H_2O/SiO_2 = 1.4 and 6.4 were calcined without hydrothermal treatment (crystallization time 0 h), and their Hf content was 3.1 and 3.0 wt.%,

respectively, which were almost the same as the amount of Hf added to the precursor gel. For H_2O/SiO_2 = 1.4, the Hf content decreased to 1.0 wt.% immediately after the start of hydrothermal treatment and did not change thereafter. For H_2O/SiO_2 = 6.4, the Hf content was initially decreased to 1.4 wt.%. However, the Hf content turned to increase after 42 h, which synchronized with the relative crystallinity, shown in Fig. 4a. After 72 h, the Hf content reached a plateau at 1.9 wt.%. Therefore, it is concluded that in the synthesis using the precursor gels with H_2O/SiO_2 = 1.4 and 6.4, the crystallization was completed in 16 and 72 h, respectively.

In order to track the missing Hf that was not found in the solid samples, elemental analysis was performed by ICP-AES for the solution remaining in the PTFE container after the hydrothermal treatment for synthesis of Hf-1.4-72, Hf-6.4-42, and Hf-6.4-72. However, Hf was not detected in these liquid samples, which implied that the missing Hf was mainly contained as unquantifiable Hf species in the solid samples. To confirm this, HfO_2/DeAl-Beta was prepared by calcining a mixture of $HfCl_4$ and DeAl-Beta with Si/Hf = 100 at 580 °C. HfO_2/DeAl-Beta showed very weak diffraction lines assignable to monoclinic HfO_2, and its Si/Hf ratio analyzed by ICP-AES was higher than 1000. These results demonstrated that extra-framework Hf species was poorly quantified by ICP-AES. Whereas, as explained above, the Hf species dispersed in the precursor gel without hydrothermal treatment was quantitatively analyzed. Hence, it is considered that the missing Hf was mainly contained in the solid samples as unquantifiable Hf species such as extra-framework Hf species and that the Hf content determined by ICP-AES indicated the amount of Hf well dispersed in the zeolite framework.

Yakimov et al. [26] reported that in the synthesis of Sn-Beta, the Sn content did not depend on the water content of precursor gel and almost all of Sn in the precursor gel was incorporated into the zeolites. In contrast, it is clearly shown that in the present synthesis of Hf-Beta, the Hf content strongly depended on the water content of the precursor gel and that the high water content was favorable for incorporation of Hf into the zeolite framework. The pH of the solution remaining after the hydrothermal treatment for Hf-1.4-72, Hf-6.4-42, and Hf-6.4-72 ranged from 9 to 10. The solubility of Hf in such weakly basic aqueous solution is one to two orders of magnitude lower than that of Sn [33,34]. Considering these points, the different feature of Hf and Sn for the incorporation into the zeolite framework was attributed to the difference in solubility of Hf and Sn in basic aqueous solution. It is presumed that a part of Hf might precipitate during the hydrothermal treatment, resulting in less incorporation into the zeolite framework. Accordingly, as the water content of precursor gel increased, the amount of such precipitated Hf decreased and Hf-Beta with high Hf content crystallized.

For both types of precursor gel with H_2O/SiO_2 = 1.4 or 6.4, insufficiently crystallized samples showed poor catalytic activity for the MPV reduction of MCHOne (Fig. 4c). Hf-1.4-16, which was a highly crystallized sample, gave 27% yield of *cis*-MCHOH. Further extension of the crystallization period did not change the catalytic activity of the samples synthesized from the precursor gel with H_2O/SiO_2 = 1.4. For the samples from the precursor gel with H_2O/SiO_2 = 6.4, catalytic activity appeared with crystallization period of 42 h or longer. The activity increased as the Hf content increased, and Hf-6.4-72 gave 59% yield of *cis*-MCHOH.

Focusing on geometric isomers of MCHOH, thermodynamically favorable *trans* isomer was

preferentially produced by using aluminum isopropoxide, which is a typical homogeneous catalyst (Table 1, Entry 1). All of Hf-Beta gave thermodynamically unfavorable *cis* isomer as a predominant product (Entries 2-4). It is known that since the formation of the *cis* isomer takes more compact transition state than that for the *trans* one, the *cis* isomer is shape-selectively produced in the micropores of the ***BEA**-type structure [35]. These results clearly showed that the MPV reduction proceeded shape-selectively in the micropores of Hf-Beta samples, demonstrating that framework Hf atoms were the active sites over Hf-Beta.

Table 1 Hf content, specific surface area, and catalytic activity of Hf-Beta samples.

Entry	Sample	Hf content [a] (wt.%)	S_{BET} [b] ($m^2\ g^{-1}$)	MCHOH yield (%)		TON [c] (-)
				cis	*trans*	
1	$Al(^iPr)_3$	-	-	22	41	-
2	Hf-1.4-72	1.0	626	24	1	888
3	Hf-4.5-72	1.6	611	38	1	864
4	Hf-6.4-72	1.9	566	59	2	1091

[a]Hf content determined by ICP-AES. [b]Specific surfacea area calculated by the BET method. [c]Turnover number calculated as total amount of MCHOH (mol) per amount of Hf (mol) in a catalyst.

Acid properties of representative Hf-Beta samples were investigated by IR spectroscopy with CD_3CN as a probe molecule. From the experiments with dosing pressure of CD_3CN varied, the adsorption on Lewis acid sites was found to be saturated at dosing pressure of 200 Pa (Fig. S4). Fig. 5a compares absorption bands of C≡N stretching vibration of CD_3CN adsorbed on Hf-1.4-72, Hf-4.5-72, and Hf-6.4-72 at the dosing pressure of 200 Pa. As in an example of Hf-6.4-72 shown in Fig. S5, these spectra were deconvoluted into four components with the peaks at 2313, 2307, 2299, and 2275

cm^{-1}. Two similar peaks above 2300 cm^{-1} have been also found in adsorption of CD_3CN on Sn-Beta and attributed to the adsorption on Sn atoms in different coordination environments [36,37]. With reference to the reports on Sn-Beta, the two peaks above 2300 cm^{-1} are assigned to the adsorption on framework Hf with Lewis acid character [19,38]. The peak at 2299 cm^{-1} was attributed to adsorption on extra-framework Hf, as HfO_2/Si-Beta mainly showed an absorption peak at 2299 cm^{-1} (Fig. S6). The peak observed at 2275 cm^{-1} is assigned to adsorption on silanol groups [39,40].

The total area of the peaks at 2313 and 2307 cm^{-1} for Hf-1.4-72, Hf-4.5-72, and Hf-6.4-72 was 0.9, 1.6, and 4.0 cm^{-1}, respectively. This increasing trend indicated that as the water content of precursor gel increased, a larger number of Lewis acid sites were formed. Turnover numbers per Hf atom (TONs) of Hf-1.4-72 and Hf-6.4-72 were 888 and 1091, respectively (Table 1, Entries 2 and 4). The larger TON for Hf-6.4-72 suggested that as the water content of precursor gel increased, the proportion of Hf that acted as Lewis acid sites increased as well. This indicates that Hf was likely to be incorporated into the zeolite framework and efficiently form Lewis acid sites under H_2O-rich conditions.

To trace the evolution of framework Hf during the hydrothermal treatment, Hf-6.4-42 was also investigated by IR with CD_3CN and compared with Hf-6.4-72 (Fig. 5b). The peaks attributed to adsorption on Lewis acid sites were also observed and the total peak area of those peaks was 1.3 and 4.0 cm^{-1} for Hf-6.4-42 and Hf-6.4-72, respectively. Thus, the number of Lewis acid sites was greatly increased after 42 h. This increase coincided with those in the relative crystallinity and the Hf content (Fig. 4a and 4b).

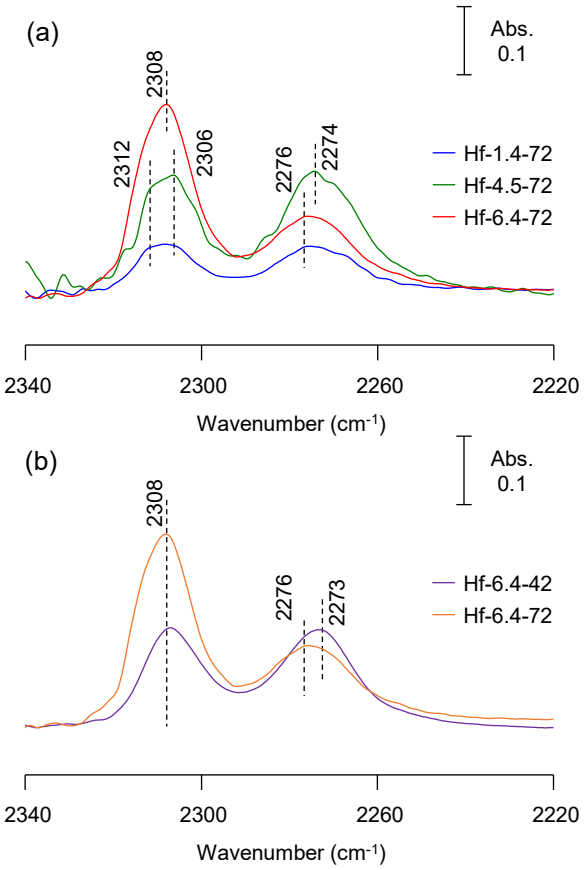

Fig. 5. FT-IR spectra of CD_3CN adsorbed on Hf-Beta (a) synthesized from precursor gel with different water content and (b) synthesized in different crystallization periods. Dosing pressure of CD_3CN was 200 Pa.

Based on the results so far, we propose the role of water in precursor gel in the hydrothermal synthesis of Hf-Beta as Fig. 6. Generally, aqueous precursor gel separated into solid and aqueous solution during hydrothermal treatment, and metallosilicate species dissolved in the solution deposited onto the solid (nuclei) together with silicate to proceed crystallization. In the present synthesis, regardless of the water content of precursor gel, the Hf content decreased sharply at the very beginning of the hydrothermal treatment and the induction period was present before increase

in the relative crystallinity (Fig. 4). It is considered that because of the low solubility of Hf species in weakly basic solution, a part of Hf species in the solution precipitated, which gave extra-framework Hf species eventually. Since such extra-framework Hf species was unquantifiable by ICP-AES, the Hf content was decreased immediately after the start of hydrothermal treatment. The induction period was attributed to the period taken for nucleation enough for the following growth of nuclei.

When the water content of precursor gel was low (H_2O/SiO_2 = 1.4), the precipitation was significant and only a limited amount of Hf in the solution was incorporated into the zeolite framework, resulting in the formation of zeolites with the low Hf content (Fig. 6a). When the water content of precursor gel was high (H_2O/SiO_2 = 6.4), Si-rich nuclei formed during the induction period and then Hf species in the solution deposited onto the nuclei in the form of hafnosilicate and Hf was effectively incorporated into the zeolite framework (Fig. 6b). As the water content of precursor gel increased, the amount of precipitated Hf species decreased and Hf-Beta with the high Hf content crystallized. Similar crystallization mechanism in which Si-rich nuclei formed first and grew with the incorporation of heteroatoms was proposed for other metallosilicate zeolites [41-43].

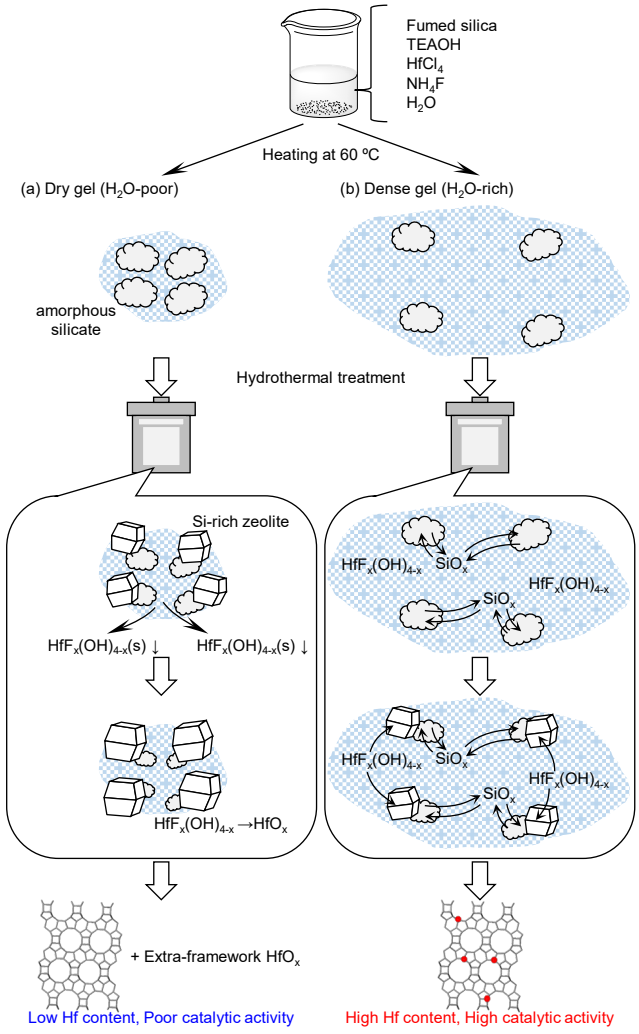

Fig. 6. Plausible mechanism for crystallization of Hf-Beta from (a) H_2O-poor or (b) H_2O-rich precursor gel.

3.3. Accelerated crystallization of Hf-Beta with assistance of seed crystal

DeAl-Beta as seed crystal (1 wt.% of SiO_2) was added to the precursor gel with H_2O/SiO_2 = 1.4 and 6.4 to accelerate the crystallization of Hf-Beta. Samples synthesized with the seed crystal are designated with "-seed" at the end of their names. From the precursor gel with H_2O/SiO_2 = 1.4 and 6.4, diffraction patterns of ***BEA**-type structure appeared in 3 and 12 h, respectively, and the induction period was significantly shortened (Figs. 7a and S7). The seed crystal promoted the

generation of nuclei during the hydrothermal treatment, so that the induction period for the nucleation was shortened. For the precursor gel with H_2O/SiO_2 = 6.4, the relative crystallinity increased sharply at 12 h, demonstrating that the growth of nuclei was accelerated by the addition of seed crystal. Even for the synthesis with seed crystal, the solid yield was ~90%, which was almost the same as that without seed.

When the precursor gel with H_2O/SiO_2 = 6.4 was used, the Hf content decreased to 1.8 wt.% in 6 h but increased after 12 h and was 2.3 wt.% after 24 h (Fig. 7b). The behavior in which the Hf content decreased once and then increased with the progress of crystallization was also observed in the synthesis without the addition of the seed crystal (Fig. 4b). The Hf content was slightly higher when seed crystal was added. It is speculated that the seed crystal provided silicate species different from that provided by fumed silica into the solution, which was prone to condense with Hf into hafnosilicate, so that the amount of Hf finally incorporated into the zeolite framework increased.

For samples from the precursor gel with H_2O/SiO_2 = 6.4, catalytic activity appeared in crystallized ones after the synthesis period of 12 h (Fig. 7c), and the yield of *cis*-MCHOH reached a maximum of 79%. This activity was higher than that of Hf-HF, which was synthesized by the conventional hydrothermal method. On the other hand, for the precursor gel with H_2O/SiO_2 = 1.4, the Hf content and catalytic activity was not increased by the addition of seed crystal.

Hf-6.4-24-seed showed the absorption peaks attributed to adsorption on Lewis acid sites and silanol groups in an IR spectrum with CD_3CN (Fig. S8). The total peak area assigned to adsorption on Lewis acid sites was 5.4 cm^{-1}. In this way, highly active Hf-Beta was successfully synthesized in

the very short period with the addition of seed crystal to the precursor gel with H_2O/SiO_2 = 6.4.

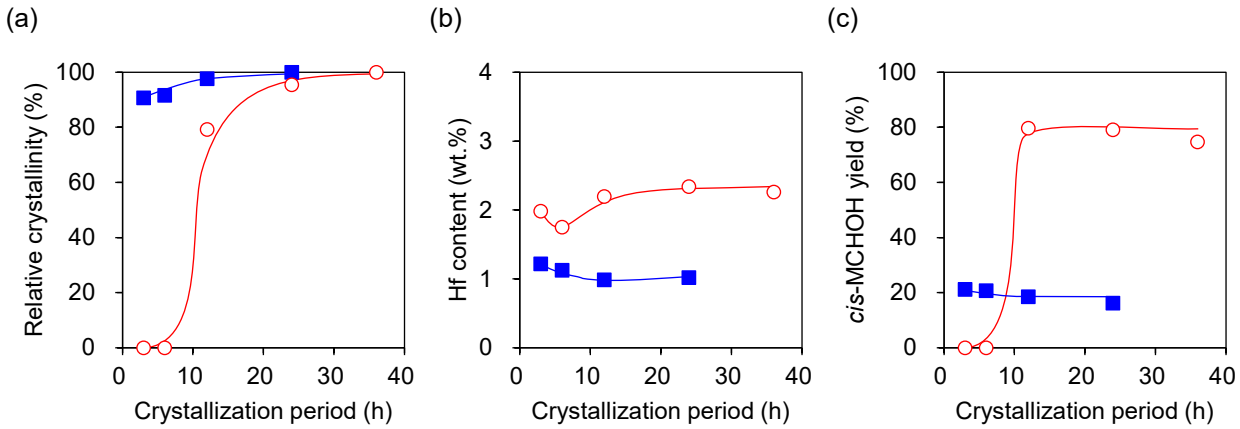

Fig. 7. Temporal changes in (a) relative crystallinity, (b) Hf content, and (c) catalytic activity for MPV reduction in course of crystallization of precursor gel containing seed crystal with H_2O/SiO_2 = 1.4 (■) and 6.4 (○). Relative crystallinity was calculated from intensity of the diffraction line at 22.7°, based on those of Hf-1.4-24-seed and Hf-6.4-36-seed, respectively. *cis*-MCHOH = *cis*-4-methylcyclohexanol.

Particle morphology of representative samples was observed by SEM. Rounded octahedral particles were observed for Hf-1.4-72 (Fig. 8a), and truncated octahedral particles typical for Beta zeolite were observed for Hf-6.4-72 (Fig. 8b). The size of both samples was ~10 μm. Hf-1.4-12-seed had spherical particles with uneven surface (Fig. 8c). For Hf-6.4-24-seed, truncated octahedral particles were majorly formed and random-shaped particles were minorly present (Fig. 8d). The particle size of these two samples was reduced to ~1 μm by the addition of seed crystal. Because the seed crystal promoted the generation of nuclei, the particle size of the grown crystal was reduced. Hf-

6.4-72 showed much higher activity than Hf-1.4-12-seed despite its larger particle size (Fig. 4c and 7c). In addition, Hf-1.4-72 and Hf-1.4-12-seed showed similar activity despite the large differences in particle size. These results implied that the catalytic activity was determined by the Hf content and the nature of Hf, independent of the particle size.

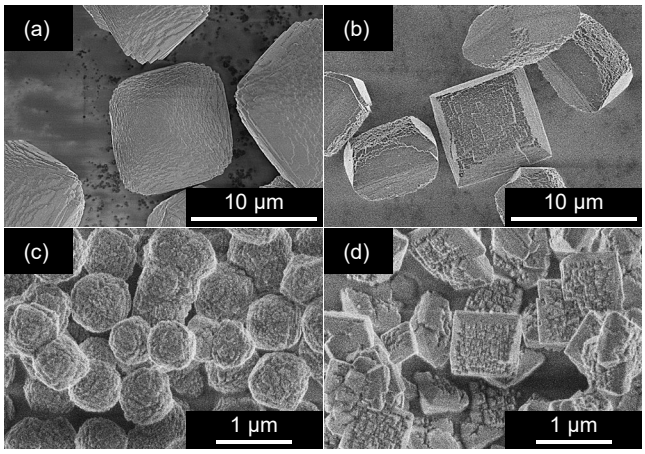

Fig. 8. SEM images of Hf-Beta. (a) Hf-1.4-72, (b) Hf-6.4-72, (c) Hf-1.4-12-seed, and (d) Hf-6.4-24-seed.

3.4. Catalytic performance of Hf-Beta for MPV reduction of various carbonyl compounds

Catalytic performance of Hf-1.4-72, Hf-6.4-72, Hf-6.4-24-seed and metallosilicate zeolites synthesized by the conventional hydrothermal method (Hf-, Zr- and Sn-HF) were compared in MPV reduction of several carbonyl compounds. (Fig. 9). In addition to MCHOne, furfural, cinnamaldehyde, and acetophenone were also used as substrates of MPV reduction. In the reaction of furfural, the corresponding acetal was also produced in addition to furfuryl alcohol. The yield of acetal was ~8% for any catalyst, which was almost the same as that in the reaction without a catalyst. The acetalization

proceeded in parallel with the MPV reduction regardless of catalysts, and so the acetal yield was excluded from the evaluation of catalytic activity. The corresponding ether was also produced in the reduction of cinnamaldehyde, and the total yield of cinnamyl alcohol and the ether was used as the product yield of MPV reduction. In the reaction of MCHOne and acetophenone, the corresponding alcohols were the sole products. Please note that reaction results of MCHOne shown in Fig. 9 are the results obtained by reducing the amount of catalyst from the standard conditions in order to suppress the conversion/product yields.

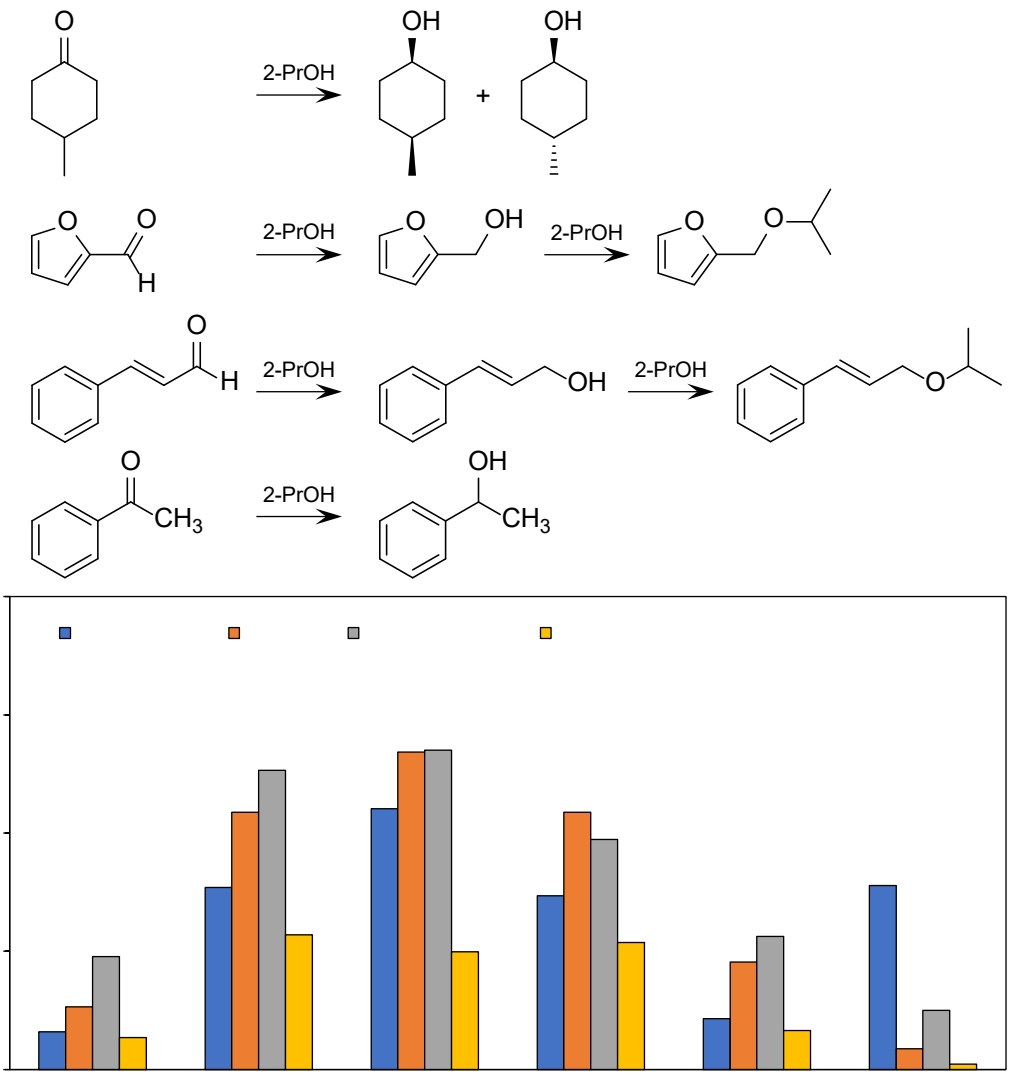

Fig. 9. Catalytic activity of Hf-Beta and other metallosilicate zeolite Beta for MPV reduction. *cis*-MCHOH = *cis*-4-methylcyclohexanol, FurOH = Furfuryl alcohol, CinOH = Cinnamyl alcohol, PhEtOH = 1-phenylethanol. Reaction conditions for MCHOne: Catalyst, 15 mg; MCHOne, 5 mmol; 2-PrOH, 10 mL; Temperature, 70 ºC; Time, 1 h. Reaction conditions for furfural: Catalyst, 25 mg; Furfural, 5 mmol; 2-PrOH, 10 mL; Temperature, 70 ºC; Time, 1 h. Reaction conditions for cinnamaldehyde: Catalyst, 100 mg; cinnamaldehyde, 5 mmol; 2-PrOH, 10 mL; Temperature, 70 ºC; Time, 1 h. Reaction conditions for acetophenone: Catalyst, 50 mg; Acetophenone, 5 mmol; 2-PrOH, 10 mL; Temperature, 70 ºC; Time, 24 h.

Hf-6.4-72 and Hf-6.4-24-seed gave much higher alcohol yields than Hf-1.4-72 for any substrate. The higher activity of Hf-6.4-24-seed and Hf-6.4-72 was due to the larger number of Lewis acid sites (Figs. 5 and S5). These two samples showed high activity for the MPV reduction of cinnamaldehyde, which is a conjugated enone, as well. Acetophenone required a long reaction time due to its significantly lower reactivity than other substrates, but Hf-6.4-24-seed and Hf-6.4-72 still showed high activity for the reduction of acetophenone.

Catalytic activity of Hf-HF, Zr-HF, and Sn-HF for MPV reduction of the three substrates except for MCHOne was decreased in the order of Hf-HF > Zr-HF > Sn-HF. On the whole, Hf-Beta showed excellent catalytic performance for MPV reduction. Turnover numbers per metal atom (TONs) for reduction of furfural of these zeolites were 840, 355, and 62, respectively (Table 2). Considering that the active sites on these Beta zeolites for MPV reduction are the framework metal atoms in common [12-18,20], the high TON of Hf-HF reflected the inherent high activity of Hf for MPV reduction. It was reported that the catalytic activity of Ti-, Zr-, and Sn-Beta for MPV reduction varied following the complex manner of electron donation/back donation between the metals and the substrates, strongly depending on the types of substrates [15]. Such a complex electronic effect could account for the exceptional high activity of Sn-Beta for the MPV reduction of MCHOne. Hf-6.4-24-seed and Hf-6.4-72 showed similar or slightly higher activity than Hf-HF synthesized by the conventional method, which demonstrated that the present method is excellent for efficiently synthesizing highly active Hf-Beta with high Hf content in a short period.

Table 2 Metal content and catalytic activity of metallosilicate zeolite samples.

Sample	Metal content [a] (wt.%)	FurOH yield [b] (%)	TON [c] (-)
Hf-1.4-72	1.0	11	381
Hf-6.4-72	1.9	44	771
Hf-6.4-24-seed	2.3	54	807
Hf-HF	1.8	44	840
Zr-HF	0.9	18	355
Sn-HF	1.3	4	62

[a]Metal content determined by ICP-AES. [b]Yield of furfuryl alcohol. [c]Turnover number calculated as amount of FurOH (mol) per amount of metal (mol) in a catalyst.

4. Conclusions

Hf-Beta samples were synthesized from precursor gel with different water content. The lower water content allowed the fast crystallization of ***BEA**-type framework. However, because of the low solubility of Hf in weakly basic solution, precipitation of Hf species was significant during the hydrothermal treatment with low water content, resulting in the less incorporation of Hf into the zeolite framework and the poor catalytic activity for MPV reduction. Thus, in order to synthesize active Hf-Beta with high Hf content, it is necessary to use precursor gel with relatively high water content, but not too high. The role of water was considered to suppress precipitation of Hf species and hold it in the form of hafnosilicate during the nucleation period. By using precursor gel with the appropriate water content (H_2O/SiO_2 = 6.4), highly active Hf-Beta zeolite was obtained in far shorter period than that required for the conventional hydrothermal method. With the assistance of seed crystal, the synthesis period was shortened to 24 h. Hf-6.4-24-seed and Hf-6.4-72 with the high Hf

content showed outstandingly high activity for the MPV reduction of several substrates and higher activity than metallosilicate zeolites that were synthesized by the conventional hydrothermal method, demonstrating that the present method is excellent for efficiently synthesizing highly active Hf-Beta with high Hf content in a short period.

Supporting Information

Detailed data on characterization of samples are available in Supporting Information.

Acknowledgements

This work was supported by JSPS KAKENHI Grant Number JP18K14052. The analysis of ICP-AES was conducted with the instrument at the Institute for Catalysis, Hokkaido University. This work was supported by Technical Division of Institute for Catalysis , Hokkaido University.

References

[1] K.G. Akamanchi, V.R. Noorani, Tetrahedron Lett. 36 (1995) 5085–5088. https://doi.org/10.1016/00404-0399(50)0946A-.

[2] R. Anwander, C. Palm, G. Gerstberger, O. Groeger, G. Engelhardt, Enhanced catalytic activity of MCM-41-grafted aluminium isopropoxide in MPV reductions, Chem. Commun. 5 (1998) 1811–1812. https://doi.org/10.1039/a802996b.

[3] E.J. Campbell, H. Zhou, S.B.T. Nguyen, Org. Lett. 3 (2001) 2391–2393. https://doi.org/10.1021/ol0162116.

[4] Y. Hua, Z. Guo, H. Han, X. Wei, Organometallics. 36 (2017) 877–883. https://doi.org/10.1021/acs.organomet.6b00921.

[5] M.A. Aramendía, V. Borau, C. Jiménez, J.M. Marinas, J.R. Ruiz, F.J. Urbano, Appl. Catal. A Gen. 206 (2001) 95–101. https://doi.org/10.1016/S0926-860X(00)00588-3.

[6] S.H. Liu, S. Jaenicke, G.K. Chuah, J. Catal. 206 (2002) 321–330. https://doi.org/10.1006/jcat.2001.3480.

[7] M. Chia, J.A. Dumesic, Chem. Commun. 47 (2011) 12233–12235. https://doi.org/10.1039/c1cc14748j.

[8] Y. Zhu, S. Jaenicke, G.K. Chuah, J. Catal. 218 (2003) 396–404. https://doi.org/10.1016/S0021-9517(03)00160-X.

[9] E.J. Creyghton, S.D. Ganeshie, R.S. Downing, H. Van Bekkum, J. Mol. Catal. A Chem. 115 (1997) 457–472. https://doi.org/10.1016/S1381-1169(96)00351-2.

[10] J.C. Van Der Waal, P.J. Kunkeler, K. Tan, H. Van Bekkum, Stud. Surf. Sci. Catal. 110 (1997) 1015–1024. https://doi.org/10.1016/s0167-2991(97)81066-x.

[11] P.J. Kunkeler, B.J. Zuurdeeg, J.C. Van Der Waal, J.A. Van Bokhoven, D.C. Koningsberger, H. Van Bekkum, J. Catal. 180 (1998) 234–244. https://doi.org/10.1006/jcat.1998.2273.

[12] A. Corma, M.E. Domine, S. Valencia, J. Catal. 215 (2003) 294–304. https://doi.org/10.1016/S0021-9517(03)00014-9.

[13] Y. Zhu, G. Chuah, S. Jaenicke, J. Catal. 227 (2004) 1–10. https://doi.org/10.1016/j.jcat.2004.05.037.

[14] Y. Zhu, G.K. Chuah, S. Jaenicke, J. Catal. 241 (2006) 25–33. https://doi.org/10.1016/j.jcat.2006.04.008.

[15] M. Boronat, A. Corma, M. Renz, P.M. Viruela, Chem. - A Eur. J. 12 (2006) 7067–7077. https://doi.org/10.1002/chem.200600478.

[16] V.L. Sushkevich, I.I. Ivanova, S. Tolborg, E. Taarning, J. Catal. 316 (2014) 121–129. https://doi.org/10.1016/j.jcat.2014.04.019.

[17] J.D. Lewis, S. Van De Vyver, A.J. Crisci, W.R. Gunther, V.K. Michaelis, R.G. Griffin, Y. Román-Leshkov, ChemSusChem. 7 (2014) 2255–2265. https://doi.org/10.1002/cssc.201402100.

[18] H.Y. Luo, D.F. Consoli, W.R. Gunther, Y. Román-Leshkov, J. Catal. 320 (2014) 198–207. https://doi.org/10.1016/j.jcat.2014.10.010.

[19] Y. Wang, J.D. Lewis, Y. Román-Leshkov, ACS Catal. 6 (2016) 2739–2744. https://doi.org/10.1021/acscatal.6b00561.

[20] M. Koehle, R.F. Lobo, Catal. Sci. Technol. 6 (2016) 3018–3026. https://doi.org/10.1039/c5cy01501d.

[21] T. Iida, K. Ohara, Y. Román-Leshkov, T. Wakihara, Phys. Chem. Chem. Phys. 20 (2018) 7914–7919. https://doi.org/10.1039/c8cp00464a.

[22] Q.H. Xia, T. Tatsumi, Mater. Chem. Phys. 89 (2005) 89–98. https://doi.org/10.1016/j.matchemphys.2004.08.034.

[23] Z. Kang, X. Zhang, H. Liu, J. Qiu, K.L. Yeung, Chem. Eng. J. 218 (2013) 425–432. https://doi.org/10.1016/j.cej.2012.12.019.

[24] Z. Kang, X. Zhang, H. Liu, J. Qiu, W. Han, K.L. Yeung, Mater. Chem. Phys. 141 (2013) 519–529. https://doi.org/10.1016/j.matchemphys.2013.05.053.

[25] L. Zhu, J. Zhang, L. Wang, Q. Wu, C. Bian, S. Pan, X. Meng, F.S. Xiao, J. Mater. Chem. A. 3 (2015) 14093–14095. https://doi.org/10.1039/c5ta02680f.

[26] A. V. Yakimov, Y.G. Kolyagin, S. Tolborg, P.N.R. Vennestrøm, I.I. Ivanova, New J. Chem. 40 (2016) 4367–4374. https://doi.org/10.1039/c6nj00394j.

[27] Q. Meng, J. Liu, G. Xiong, X. Liu, L. Liu, H. Guo, Microporous Mesoporous Mater. 266 (2018) 242–251. https://doi.org/10.1016/j.micromeso.2018.02.040.

[28] Q. Meng, J. Liu, G. Xiong, X. Li, L. Liu, H. Guo, Microporous Mesoporous Mater. 287 (2019) 85–92. https://doi.org/10.1016/j.micromeso.2019.05.059.

[29] Y. Luo, Y. Zhu, J. Pan, X. Chen, Green Chem. 22 (2020) 1681–1697. https://doi.org/10.1039/c9gc03869h.

[30] Q. Meng, J. Liu, G. Xiong, L. Liu, H. Guo, Microporous Mesoporous Mater. 294 (2020) 109915. https://doi.org/10.1016/j.micromeso.2019.109915.

[31] X. Yang, L. Wang, T. Lu, B. Gao, Y. Su, L. Zhou, Catal. Sci. Technol. 10 (2020) 8437–8444. https://doi.org/10.1039/d0cy01625j.

[32] R. Otomo, R. Kosugi, Y. Kamiya, T. Tatsumi, T. Yokoi, Catal. Sci. Technol. 6 (2016) 2787–2795. https://doi.org/10.1039/c6cy00532b.

[33] D. Rai, Y. Xia, N.J. Hess, D.M. Strachan, B.P. McGrail, J. Solution Chem. 30 (2001) 949–967. https://doi.org/10.1023/A:1013337925441.

[34] D. Rai, M. Yui, H.T. Schaef, A. Kitamura, J. Solution Chem. 40 (2011) 1155–1172. https://doi.org/10.1007/s10953-011-9723-1.

[35] J.C. Van Der Waal, E.J. Creyghton, P.J. Kunkeler, K. Tan, H. Van Bekkum, Top. Catal. 4 (1997) 261–268. https://doi.org/10.1023/a:1019160827175.

[36] M. Boronat, P. Concepción, A. Corma, M. Renz, S. Valencia, J. Catal. 234 (2005) 111–118. https://doi.org/10.1016/j.jcat.2005.05.023.

[37] J.S. Bates, B.C. Bukowski, J.W. Harris, J. Greeley, R. Gounder, ACS Catal. 9 (2019) 6146–6168. https://doi.org/10.1021/acscatal.9b01123.

[38] S. Rojas-Buzo, P. Concepción, A. Corma, M. Moliner, M. Boronat, ACS Catal. 11 (2021) 8049–8061. https://doi.org/10.1021/acscatal.1c01739.

[39] B. Wichterlová, Z. Tvarůžková, Z. Sobalík, P. Sarv, Microporous Mesoporous Mater. 24 (1998) 223–233. https://doi.org/10.1016/S1387-1811(98)00167-X.

[40] J. Penzien, A. Abraham, J.A. Van Bokhoven, A. Jentys, T.E. Müller, C. Sievers, J.A. Lercher, J. Phys. Chem. B. 108 (2004) 4116–4126. https://doi.org/10.1021/jp0373043.

[41] W. Fan, R.G. Duan, T. Yokoi, P. Wu, Y. Kubota, T. Tatsumi, J. Am. Chem. Soc. 130 (2008) 10150–10164. https://doi.org/10.1021/ja7100399.

[42] S. Tolborg, A. Katerinopoulou, D.D. Falcone, I. Sádaba, C.M. Osmundsen, R.J. Davis, E. Taarning, P. Fristrup, M.S. Holm, J. Mater. Chem. A. 2 (2014) 20252–20262.

https://doi.org/10.1039/c4ta05119j.

[43] P.A. Kots, A. V. Zabilska, E. V. Khramov, Y. V. Grigoriev, Y. V. Zubavichus, I.I. Ivanova, Inorg. Chem. 57 (2018) 11978–11985. https://doi.org/10.1021/acs.inorgchem.8b01548.